Microfluidics and Nanofluidics (2021) 25:75
https://doi.org/10.1007/s10404-021-02475-2

RESEARCH PAPER

Effects of sample rheology on the equilibrium position of particles and cells within a spiral microfluidic channel

Mohammad Amin Raoufi[1,2,3] · Hossein Ahmadi Nejad Joushani[1] · Sajad Razavi Bazaz[1] · Lin Ding[1] · Mohsen Asadnia[2] · Majid Ebrahimi Warkiani[1,4]

Received: 5 April 2021 / Accepted: 27 July 2021

Abstract

Elasto-inertial migration in non-Newtonian fluids is a rapidly growing field with tremendous potentials for manipulating micron to submicron particles. Previous research attempts were mainly carried out in straight channels due to the complexity of particle migration, solution tuning, and data analysis in elasto-inertial microfluidics. Consequently, the combined effects of Dean drag force and solution rheology on coupled Dean drag elasto-inertial focusing phenomena have not been carefully analyzed. This study delved thoroughly into the combined effects of solution rheology and Dean drag force on elasto-inertial focusing of particles and cells within a spiral microchannel. Polyethylene oxide (PEO) of 1MDa, 2MDa, and 4MDa molecular weights were used to prepare 250, 500, and 1000 ppm non-Newtonian solutions to investigate the focusing behavior of particles and cells over a wide range of flow rates and solution rheologies. Dean coupled elasto-inertial effects were systematically investigated to demonstrate its potentials for position-adjustable and size-tunable particle and cell focusing phenomenon. Various cells and microbeads with diameters ranging from 1 to 17 µm were employed to carefully study the equilibrium position, focusing band, and migration behavior under different elastic, inertial, and Dean conditions. Following the focusing, cell viability, morphology, and growth rate were evaluated which showed cells remained undamaged from viscosity, shear rate, and chemical properties of PEO solutions. We are of the opinion that the current study can provide scientists with a better understanding of focusing phenomena in viscoelastic fluids within spiral microfluidic channels.

Keywords Elasto-inertial microfluidics · Solutions rheology · Non-Newtonian fluids · Microchannels · Particle focusing

1 Introduction

Inertial microfluidics has received significant interest in the microfluidic community owing to its numerous merits such as enhanced particle control and manipulation, low-cost, and low volume sample (Mihandoust et al. 2020). This technology has been widely used for a variety of biological and biomedical applications, including cell/particle sorting and separation (Warkiani et al. 2015b; Rzhevskiy et al. 2020), particle focusing and filtration (Moloudi et al. 2018; Warkiani et al. 2015a; Raoufi et al. 2019), and sample mixing (Razavi Bazaz et al. 2020a). However, inertial-based approaches have been less effective for focusing of micron/submicron particles (less than ~ 3 µm) since the inertial forces are strongly dependent on particle size (Seo et al. 2014a). Recent investigations prove that elasto-inertial focusing is an appropriate alternative to the inertial-based methods due to the presence of an extra elastic lift force (Liu et al. 2016, 2017) and intriguing inherent characteristics

Mohammad Amin Raoufi, Hossein Ahmadi Nejad Joushani and Sajad Razavi Bazaz have contributed equally to this work as the first author.

✉ Majid Ebrahimi Warkiani
majid.Warkiani@uts.edu.au

[1] School of Biomedical Engineering, University of Technology Sydney, Ultimo, NSW 2007, Australia

[2] School of Engineering, Macquarie University, Sydney, NSW 2109, Australia

[3] Department of Mechanical Engineering, Ferdowsi University of Mashhad, Mashhad, Iran

[4] Institute of Molecular Medicine, Sechenov First Moscow State University, Moscow 119991, Russia

Published online: 10 August 2021

of non-Newtonian solutions (Raoufi et al. 2020). In elasto-inertial microfluidics, micron to submicron particles can be effortlessly manipulated without the need for any external forces or components. Accordingly, high-resolution particle focusing and separation are simply achievable with low cost and high versatility.

Many industrial products, biological samples (e.g., blood, plasma, and DNA solution), and chemical fluids exhibit non-Newtonian properties. Recently, specific polymers such as polyethylene oxide (PEO), polyvinylpyrrolidone (PVP), polyacrylamide (PAA), and xanthan gum (XG) have been extensively used to prepare non-Newtonian solutions. By mixing these long-chain polymers with Newtonian fluids, the nonlinear behavior of viscosity, either shear thickening or shear thinning, can be stimulated. In non-Newtonian solutions, particles experience first and second normal stress differences that cause a cross-stream migration and secondary flows perpendicular to the main flow, respectively. The second normal stress effects are much smaller than the first normal stress for most non-Newtonian solutions, and the elastic force stems from the first normal stress. Generally, in elasto-inertial focusing, the particle migration is dominated by combined effects of elasticity and inertia, which can culminate in a higher throughput in case of a proper balance between elastic and inertial forces. By balancing the competition among the elastic and inertial forces, an adjustable focusing band can be achieved by changing the solution's rheological properties, which is a desirable demand for numerous microfluidic applications.

The earliest research on solution rheology was conducted by Leshansky et al. (2007). They demonstrated that an ultra-diluted PAA solution could enhance the particle focusing in a shallow straight rectangular channel. Later, Seo and colleagues (2014a, 2014b) explored the effect of shear-thinning fluids on particle migration in a tube and a rectangular channel for PEO (4 MDa) and PVP (360 kDa) solutions. They discovered that aligned particles at the channel center began to disperse by increasing the flow rate due to the decrease in the viscosity caused by the substantial shear-thinning property of the solution. Following this finding, several studies were carried out to explore the effect of rheological parameters (i.e., polymer length, relaxation time, molecular weight, concentration) on the particle focusing (Yang et al. 2011; Xiang et al. 2016a; Ahn et al. 2015; Holzner et al. 2017). Results showed that solutions with shorter polymer length and lower molecular weight can lead to a tighter focusing band (Song et al. 2016). Nonetheless, microfluidic devices used in the abovementioned studies were predominately straight microchannels, chosen for their simplicity in operation, data analysis, and particle manipulation.

Additional Dean drag in curved channels previously showed constructive effects on the particle focusing in elasto-inertial systems (Lee et al. 2013). Among these channels, the spiral design has shown greater potential for high-throughput particle sorting due to the formation of more uniform and unidirectional Dean drags, and few studies have been carried out to investigate the applications and fundamentals of elasto-inertial focusing in spiral channels (Xiang et al. 2016b, 2018; Kim et al. 2018, 2019; Yuan et al. 2019; Zhou et al. 2020). In 2016, Xiang et al. (2016b) studied the physics of particle focusing in curved channels. They proposed a six-stage process model to explain the particle focusing phenomenon in Dean-coupled elasto-inertial systems. However, they only evaluated the effects of flow rate channel aspect ratio and channel radii on the focusing phenomenon, while in non-Newtonian systems, elasticity plays an undeniable role in lateral migration of particles. Recently, new curved channels with various features and cross-sections have been introduced to increase the efficiency and throughput of particle sorting in non-Newtonian fluids (Raoufi et al. 2020; Tang et al. 2019). Lu et al. (2021) proposed a novel curved microchannel and managed to separate bacteria from blood cells at a flow rate of 102 µl/min. However, the bacteria recovery rate was around 80%, showing the entire system still needs more modification and improvements. Kumar et al. (2021) separated 10 and 15 µm particles at the flow rate of 1 ml/min by tuning the elasticity and inertial effects. In another study, Tang et al. (2021) used an asymmetric serpentine channel to accurately characterize tumor cells and blood cells. In addition to these sheathless devices, lately, very few studies performed on the coflow elasto-inertial systems in curved channels (Nikdoost and Rezai 2020; Iyengar et al. 2021). Nevertheless, all these efforts mainly evaluated the effects of geometry, flow rates, and blockage ratio on particle migration. Despite the importance of solution rheology on particles and cells focusing behavior, few studies investigate the underlying mechanisms of particles and cells focusing within Dean-coupled elasto-inertial microfluidic devices. Besides, selecting the proper molecular weight and solution concentration for each application is an important factor. Nonetheless, a general decision-making guideline for Dean-coupled elasto-inertial microfluidic systems is not available.

Herein, a comprehensive framework for implementing non-Newtonian solutions to manipulate a wide range of particles and cells is presented. The underlying physics of Dean-coupled elasto-inertial migration was explored entirely within a spiral microfluidic channel. First, the focusing behavior of 3 µm particles was examined. Then, the effects of Dean drag force, PEO molecular weight, and PEO solution concentration on the focusing pattern of 3 µm particles were analyzed. After a comprehensive experimental investigation and careful optimization of the inertial, elastic, and Dean drag forces, the optimum flow rates and solutions rheology in which there was a tight focusing band for 3 µm particles were obtained. These findings were explored over

a wide range of cells, from HeLa to yeast, and extended to 1 μm particles. To show the capability of the presented guidelinein clinical studies, HeLa cells were proceeded through the device to investigate the effects of non-Newtonian solutions on cell viability, morphology, and growth rate. Benefiting from the presented framework, particles and cells can be easily driven to the proposed sheathless Dean-flow coupled elasto-inertial device and strongly aligned at different locations of the spiral microchannel (Fig. 1). As shown in Fig. 1B, particles of different sizes are randomly introduced into the system and precisely aligned in some specific locations near the outlet according to the channel size, solution rheology, and flow rate.

2 Materials and method

2.1 Solution preparation

To analyze the effects of rheology on particle migration, 250, 500, and 1000 ppm PEO solutions (Sigma-Aldrich, Australia) with 1, 2, and 4 MDa molecular weights were prepared by adding 0.0125, 0.025, and 0.05 gr of PEO polymers to a 50 ml MACS buffer, respectively. The rotational rheometer cannot measure the relaxation time at these concentrations because of the low value of shear viscosities. Therefore, the empirical relaxation time was

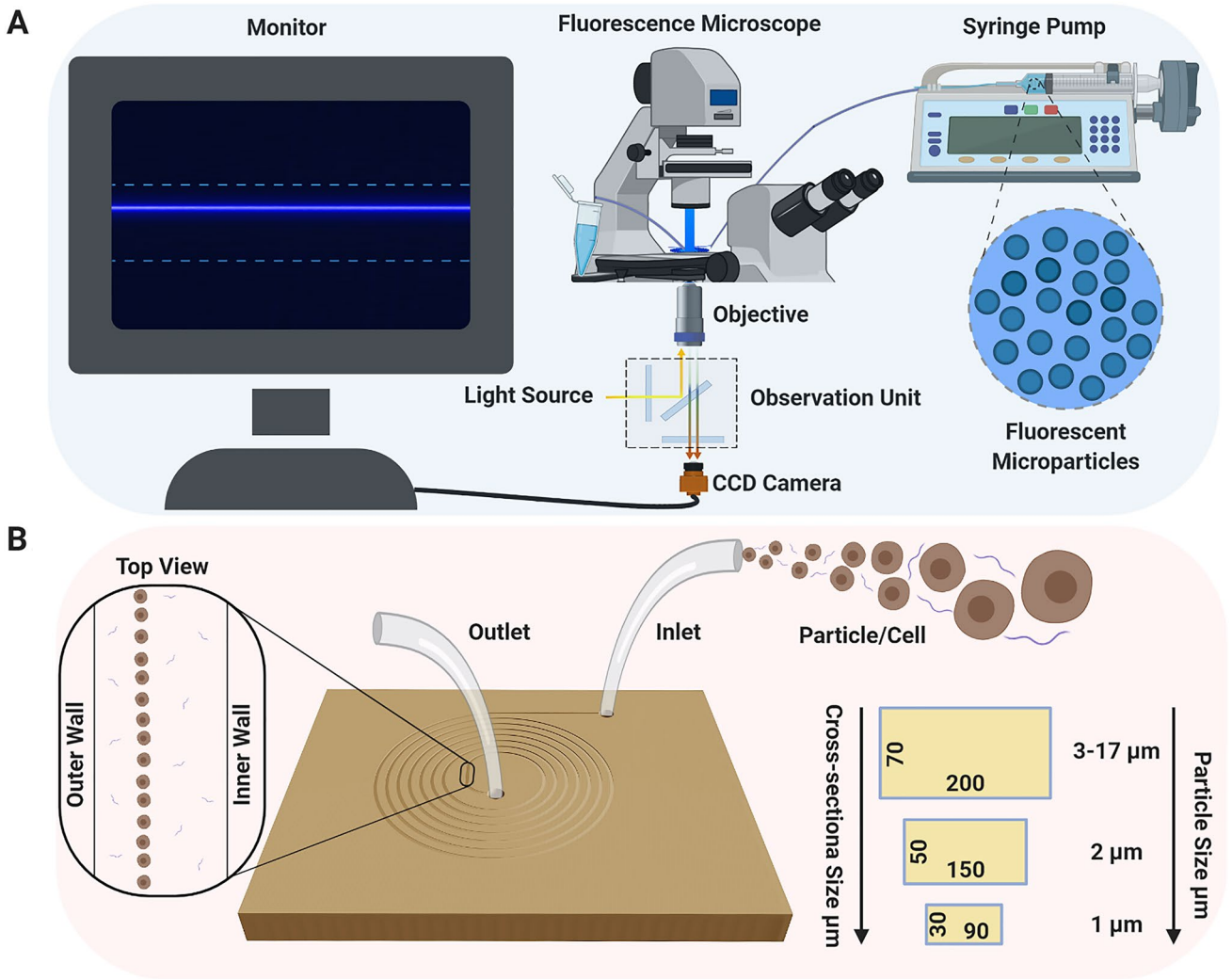

Fig. 1 **A** Schematic of the setup used to run the experiments and visualize the results. The sheathless Dean-flow coupled elasto-inertial system to systematically investigate Dean-couple elasto-inertial microfluidics and demonstrate its capability for position-adjustable and size-tunable particles and cells focusing. Samples were easily loaded into a 5 ml BD plastic syringe and injected into the microchannel using a syringe pump. The plastic tubes were used for the microchannel inlet and outlet, and the results were captured using a CCD camera. **B** Schematic illustration of cell/particle being focused in the spiral microchannel with depicted cross-sectional dimensions. A rectangular spiral channel with seven loops and different cross-sections (200 μm × 70 μm, 150 μm × 50 μm, and 90 μm × 30 μm) was used to achieve a tight focusing band for different cells and particles at the optimum flow rates and solutions rheology

implemented based on the Zimm theory as follows (Rodd et al. 2005, 2007):

$$\lambda_{Zimm} = \frac{f[\eta]M_w\eta_s}{RT} \quad (1)$$

Here, f, $[\eta]$, M_w,η_s, R, T are a solvent quality factor, intrinsic viscosity, molecular weight, solvent viscosity, gas constant, and absolute temperature, respectively. The empirical relaxation time is $\lambda_e = 18\lambda_{Zimm}(c/c^*)^{0.65}$ where c and c* are the polymer concentration and the overlapping polymer concentration, respectively. For the PEO solutions considered here, the f value is considered to be 0.463 (Rodd et al. 2005; Tirtaatmadja et al. 2006), and T is 295 K. Other properties are provided in Table 1.

Later, 1, 2, and 3 µm fluorescent polystyrene particles (Magsphere-Pasadena, California) were added to the PEO solutions to make 5×10^4 particle/ml concentration. Furthermore, Saccharomyces cerevisiae cells (Sigma-Aldrich, Australia), Red Blood Clls, and HeLa cells were added to the optimized PEO solutions (1000 ppm 1MDa and 500 ppm 4MDa) to make approximately 3 million cells/ml.

2.2 Experimental setup

The prepared PEO solutions were loaded into a 5 ml BD plastic syringe and injected through the channel by a syringe pump (Chemyx Fusion 200, Chemyx, TX, USA). After connecting the inlet and outlet tubes, the channel was fixed on the stage of an inverted fluorescence microscope (IX73, Olympus, Tokyo, Japan). To visualize the focusing of particles and cells, bright-field and fluorescent images were captured by a high speed (Phantom- VEO 640L) and a CCD camera (DP80, Olympus, Tokyo, Japan), respectively. The microscope objective and the exposure time were set to 10X and 60 µs for bright-field imaging and 10X and 800 ms for fluorescent microscopy. All the analysis and post-processing on the captured photos have been performed by ImageJ software.

2.3 Device structure and fabrication

In this research, a rectangular spiral channel with seven loops was fabricated to investigate the effects of rheology on the particle focusing behavior within a Dean-flow-coupled elasto-inertial microchannel. The spiral channel has an inner diameter of 1.2 cm and a width and height of 200 and 70 µm, respectively. The channel was fabricated via a soft lithography technique on a 3D printed master mold. The spiral mold was first drafted by a commercial CAD drawing software (SolidWorks 2016) and saved as an STL format to make it readable for the digital light processing (DLP) 3D printer (MiiCraft Ultra 50, MiiCraft, Hsinchu, Taiwan). The design mold was then sliced in the Z direction using the Miicraft software (Version 4.01, Miicraft) (Razavi Bazaz et al. 2019). The mold was fabricated layer by layer on a picker when the UV light projected from the bottom of the resin bath (filled with BV-007 resin) and passed through a transparent Teflon film. When the spiral mold was printed completely and removed from the picker, it was washed with isopropanol (IPA) multiple times and dried with an air-gun, followed by a post-curing for 5 min using a UV-cure chamber. Then, the mold was soaked into IPA for 4 h to remove the uncured monomers and oligomers on the surface, and again, it was washed and dried. Following this, oxygen plasma treatment (Basic Plasma cleaner PDC-002, Harrick Plasma) was conducted for 6 min, and the surface of the mold was salinized using trichloro (1H, 1H, 2H, 2H-perfluoro-octyl) saline (Sigma-Aldrich, Australia) in a desiccator under vacuum for 6 h to make the PDMS replication process easier (Shrestha et al. 2019). Please check our previous publication for the detailed procedure (Bazaz et al. 2020).

2.4 Elasto-inertial cell sorting

Two different sets of experiments were conducted to evaluate the effects of the non-Newtonian solution on the cell viability, morphology, and growth rate. The aim of the first set of experiments was to investigate the effects of non-Newtonian

Table 1 Composition and properties of PEO solutions obtained at various molecular weights and concentrations

M_w (g/mol)	c (ppm)	[η] (ml/g)	c/c^*	η_s (pa.s)	λ_{zimm} (s)	λ_e (s)
1×10^6	250	5.72×10^2	0.15	0.0034	3.7×10^{-4}	1.9×10^{-3}
1×10^6	500	5.72×10^2	0.31	0.0034	3.7×10^{-4}	3.1×10^{-3}
1×10^6	1000	5.72×10^2	0.62	0.0034	3.7×10^{-4}	4.8×10^{-3}
2×10^6	250	8.97×10^2	0.24	0.0034	1.2×10^{-3}	8.5×10^{-3}
2×10^6	500	8.97×10^2	0.48	0.0034	1.2×10^{-3}	0.013
2×10^6	1000	8.97×10^2	0.96	0.0034	1.2×10^{-3}	0.021
4×10^6	250	1.38×10^3	0.26	0.0034	3.59×10^{-3}	0.027
4×10^6	500	1.38×10^3	0.52	0.0034	3.59×10^{-3}	0.042
4×10^6	1000	1.38×10^3	1.04	0.0034	3.59×10^{-3}	0.066

solutions on cell morphology. In the second set of experiments, the viability of the cell was evaluated using flow cytometry technique. In each set of experiments, three different samples were used: the control sample, the 1MDa solution with 1000 ppm PEO solution with 1MDa molecular weight, and 500 ppm PEO solution with 4MDa molecular weight.

2.5 Cell culture

HeLa cell lines were recovered from – 80 °C freezer, seeded in T-25 flasks with 90% RMPI-1640 media (Invitrogen, Australia) and 10% Fetal Bovine Serum supplementary (Invitrogen, Australia) and cultured for two days. When the cells reached 80–90% confluence, the TrypLE enzyme (Invitrogen, Australia) was used to harvest the cells. Cells were washed by DPBS, and then the DPBS was replaced by 1000 ppm PEO 1MDa, and 500 ppm PEO 4MDa.

2.6 Flow cytometry

The cells proceeded through the device at the flow rates of 50, 125 µL/min in 1MDa solution, and at the flow rates of 10, 50 µL/min in 4MDa solution. The cells were collected and centrifuged at 500*g* for 5 min to replace the non-Newtonian solutions with 200 µL DPBS. Then, 0.4 µL of live and dead staining (Abcam, Australia) was added into each cell group, and the cells were proceeded through Cytoflex LX (Beckman Coulter, U.S.) flow cytometer. The counting was repeated in triplets.

2.7 Growth rate and morphology observation

The control sample was cultured without passing through the device, whereas 1MDa and 4MDa samples were cultured after passing through the device. For the 1MDa and 4MDa groups, the flow rates of 50 and 125 µl/min (based on the optimum results) were used. Three groups of cells were counted and seeded in a 12-well plate (Corning, Australia) with a low concentration to better observe the growth rate (0.1×10^5). The pictures of the cells were recorded by an inverted fluorescence microscope every 24 h. The area covered by cells was measured using ImageJ. The increase of cell coverage area on the plate was calculated to evaluate the growth rate of cells affected by Non-Newtonian solutions. Three areas for each group were recorded every day.

3 Physics of elasto-inertial focusing in spiral channels

Particle migrations and trajectories in non-Newtonian fluids in spiral microchannels are controlled by three hydrodynamic forces; elastic, net inertial, and Dean drag. Taking advantage of these forces, spiral devices can precisely focus microparticles at high flow rates. In non-Newtonian solutions, the elastic force (F_E) originating from the asymmetric normal stress differences on the particle surface directs particles towards the lowest shear stress regions (Huang et al. 1997). In these fluids, the first normal stress difference ($N_1 = \tau_{11} - \tau_{22}$) causes a cross-stream migration, while the second normal stress difference ($N_2 = \tau_{22} - \tau_{33}$) tends to create secondary flows perpendicular to the main flow (Bird et al. 1987; Villone et al. 2013), where τ_{11}, τ_{22} and τ_{33} are in the flow, velocity gradient, and vorticity directions, respectively. The net inertial force generally comprised of wall-induced and shear gradient lift forces directing particles towards the channel center and walls, respectively. The Dean drag force resulting from a sharp pressure gradient between the inner and outer wall in curved channels can also affect particle equilibrium position. For a Dean-flow-coupled elasto-inertial system with rectangular cross-section, the elastic, net inertial, and Dean forces can be obtained by the following equations (Xiang et al. 2016b):

$$F_{Elastic} \sim 8a_p^3 \lambda \left(\frac{Q}{hw^2} \right)^3 \tag{2}$$

$$F_{Inertial} \sim \frac{1}{4} \rho Q^2 a_p^4 \left(\frac{(w+h)^2}{(hw)^4} \right) \tag{3}$$

$$F_{Drag} \sim \frac{4\rho Q^2 a_p}{R(w+h)^2} \tag{4}$$

where a_p, λ, Q, ρ, h, w, and R are the particle size, the relaxation time of non-Newtonian solution, flow rate, fluid density, channel height, channel width, and channel curvature radius, respectively. Elastic and Dean drag forces can be estimated by non-dimensional numbers to simplify the calculations. The strength of the Dean drag can be expressed by Dean number (*De*) as follows (Xiang et al. 2016b; Razavi Bazaz et al. 2020b):

$$De = Re\sqrt{D_h/2R} \tag{5}$$

with D_h being the channel hydraulic diameter that for rectangular channels can be expressed as $D_h = 2wh/(w+h)$. According to these equations, decreasing the curvature radius augments the Dean drag. Elastic force (F_E) can also be estimated by introducing the Weissenberg number (*Wi*) as below (Xiang et al. 2016b):

$$Wi = \lambda \dot{\gamma}_c = \frac{2\lambda Q}{hw^2} \tag{6}$$

with λ being the relaxation time of non-Newtonian fluids, and $\dot{\gamma}_c$ is the characteristic shear rate, which can be defined as $\dot{\gamma}_c = 2Q/hw^2$ for rectangular microchannels.

It is noteworthy that channel dimension, solution rheology, aspect ratio, particle size, and Reynolds number ($Re = \rho v_t a_p/\mu$, v_t is the relative velocity of the fluid to particle) are the foremost factors controlling the particle migration in the elasto-inertial microfluidic devices. Moreover, the particle diameter (a_p) and flow rate noticeably affect the elastic, inertial, and drag forces due to the strong interrelation between them. Consequently, particles with different sizes are assumed to migrate with different lateral velocities, making spiral channels suitable for size-dependent separation.

To illustrate the focusing phenomenon and underlying physics in a Dean-flow-coupled elasto-inertial spiral microchannel, Fig. 2A compares the focusing pattern of 3 µm particles in a Newtonian and highly diluted non-Newtonian solution (1 MDa PEO with 250 ppm concentration). Then, Fig. 2B and C demonstrate the focusing behaviors in different PEO solutions (1, 2, and 4MDa molecular weight with 250 ppm concentration) through the channel to explain the combined effects of Dean and solution rheology. According to Fig. 2A, in the Newtonian solution, particles are scattered for all tested flow rates while migrating slightly towards the inner wall for Q > 100 µl/min. This occurs because the pure inertial force at this blockage ratio (ap/DH ≈ 0.03) is insufficient to sort 3 µm particles. Nevertheless, by increasing the flow rate, more than 100 µl/min, Dean flows form and direct particles towards the inner wall where inertial and Dean drag forces can weakly balance each other. By increasing the flow rate to 200 µl/min, Dean drag force dominates the opposing inertial force, resulting in the dispersion of particles. However, focusing patterns in 1 MDa PEO solution demonstrate that even weak viscoelasticity can noticeably alter the focusing position. As demonstrated in Fig. 2A, particles start to migrate towards the outer wall even at a low flow rate of 10 µl/min. Additionally, by exceeding 100 µl/min, the focusing band shifts towards the channel center due to the augmentation of the inertial force and starts to disperse when approaching 200 µl/min. To elucidate the focusing patterns within the Dean-flow coupled elasto-inertial system, the cross-section of the spiral channel is divided into three regions, which determine the force balance (Fig. 2C). As shown in the region (I), wall-adjacent particles first move outwards due to the elastic and inertial forces and then are dragged towards the center and outer wall by Dean drag force. Since all forces in this region act unidirectionally, there was no stable focusing position near the inner wall. On the other hand, in region (II), Dean drag force and shear gradient lift force can balance the opposing elastic and wall-induced lift forces, causing particles to focus near the outer wall. Unfocused particles return to the inner wall from sidewall (regions (III)), where Dean drag is perpendicular to elastic and inertial forces, which impede particle focusing.

Achieving a tight focusing band at high throughputs requires accurate control of elasticity, inertia, and Dean effects. Furthermore, the shear-thinning effect in non-Newtonian solutions plays a dominant role in dispersing particles and needs to be precisely controlled since the shear-thinning property can cause pre-aligned particles to disperse (Liu et al. 2015; Ahn et al. 2015). Due to the complexity of particle focusing behavior in non-Newtonian microfluidic devices and combined effects of shear-thinning and Dean effects on focusing, these parameters will be experimentally investigated in the following sections.

4 Viscoelastic fluids in spiral inertial microfluidics

4.1 Dean flow effects

In spiral microchannels, Dean drag force contributes significantly to particle migration at moderate flow rates. Figure 2B depicts particle trajectories captured at a specific position in each loop of the spiral channel. PEO solutions with different molecular weights, but same concentration (500 ppm), was utilized to investigate how Dean drag can be tuned by viscoelasticity. Notably, for the 1MDa solution at a flow rate of Q = 100 µl/min, particles gradually move towards the channel outer wall due to the synergetic effects of elasticity and Dean drag effects. However, this condition is not optimal for achieving a tight focusing band, as the opposing inertial force dominates the Dean force, causing particles to remain dispersed at the central region of the channel. It should be noted that the Dean force becomes stronger along the channel length due to the continual decrease in the radius of the channel curvature. According to Eq. 5, the Dean number ratio between loop 7 and 1 $\left(De_{7\text{th}}/De_{1th} = \sqrt{R_{1th}/R_{7th}}\right)$ is 1.22 indicating an increase in the Dean drag force throughout the channel length where this growth tightens the focusing band near the outer wall.

Moreover, under the same flow rate, increasing the molecular weight modifies the Dean drag and inertial effects. For example, increasing the molecular weight from 1MDa to 2 and 4 MDa enhances the particle focusing near the outer wall. This improvement can be attributed to the surge of the elastic force arising from an increase in the molecular weight or polymer length, which would intensify the relaxation time; consequently, increase the Wi ($wi \propto \lambda_d$) number. Further, as mentioned earlier, the Dean drag force gradually increases throughout the channel length, causing the focusing band to become steadily tighter in the last loop. Nevertheless, there always remain some unfocused particles

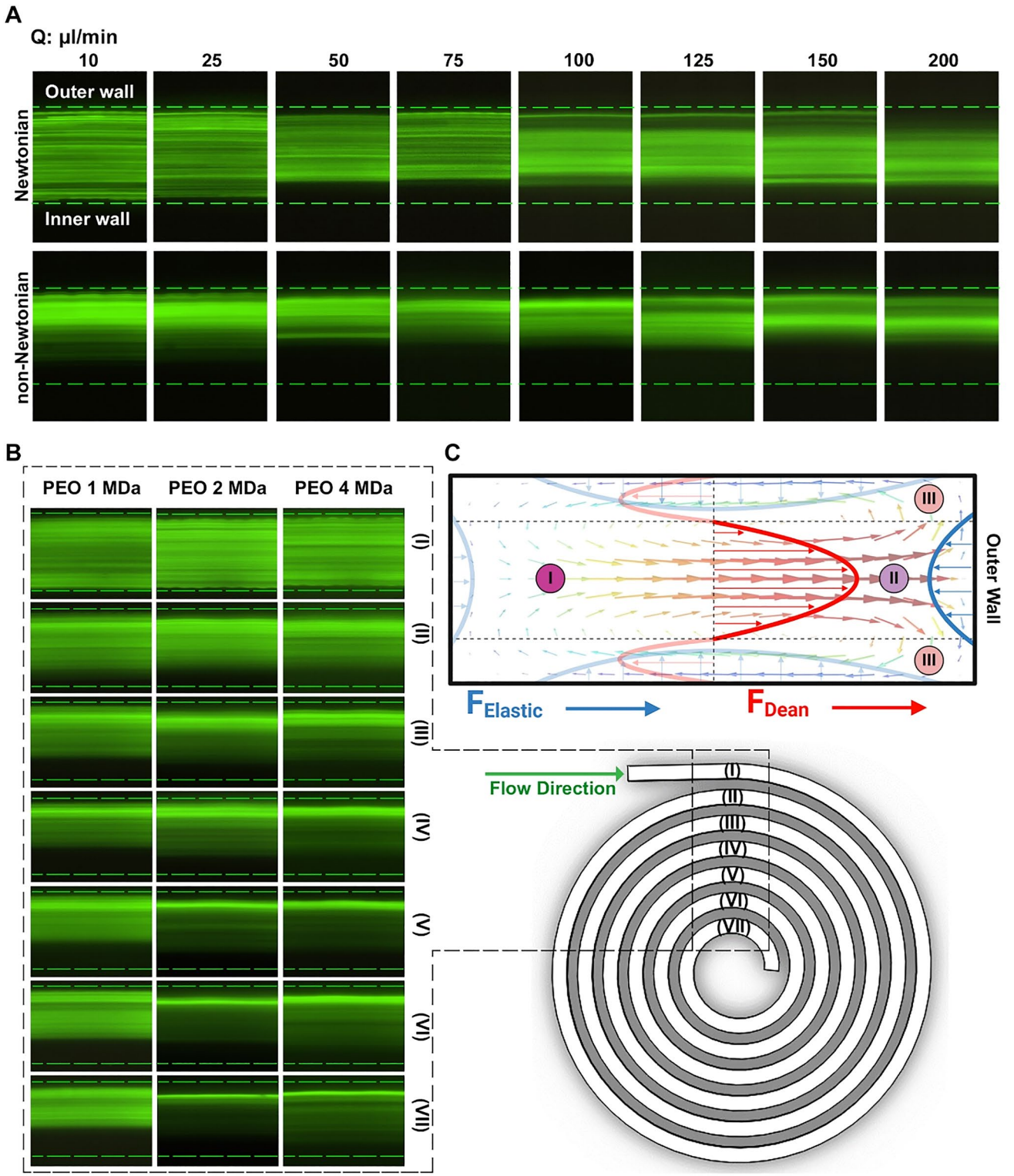

Fig. 2 **A** Focusing positions of 3 µm particles in Newtonian (MACS Buffer) and non-Newtonian (1 MDa PEO with 250 ppm concentration) solutions within a Dean-flow-coupled elasto-inertial spiral microchannel. Top view illustrates the focusing positions at the channel outlet over a wide range of flow rates. **B** Particle trajectories at specific positions throughout the length of spiral channel in each loop for 500 ppm PEO solutions with different molecular weights (1, 2, and 4MDa) at a flow rate of 100 µl/min. **C** Schematic of the forces applied on particles in a Dean-coupled elasto-inertial microfluidic channel. The cross-section of the spiral channel is divided into three regions; the region (I) in which all forces act unidirectionally, the region (II) where the Dean drag force and shear gradient lift force can balance the opposing elastic and wall-induced lift forces, and the regions (III) in which the Dean drag force is perpendicular to elastic and inertial forces

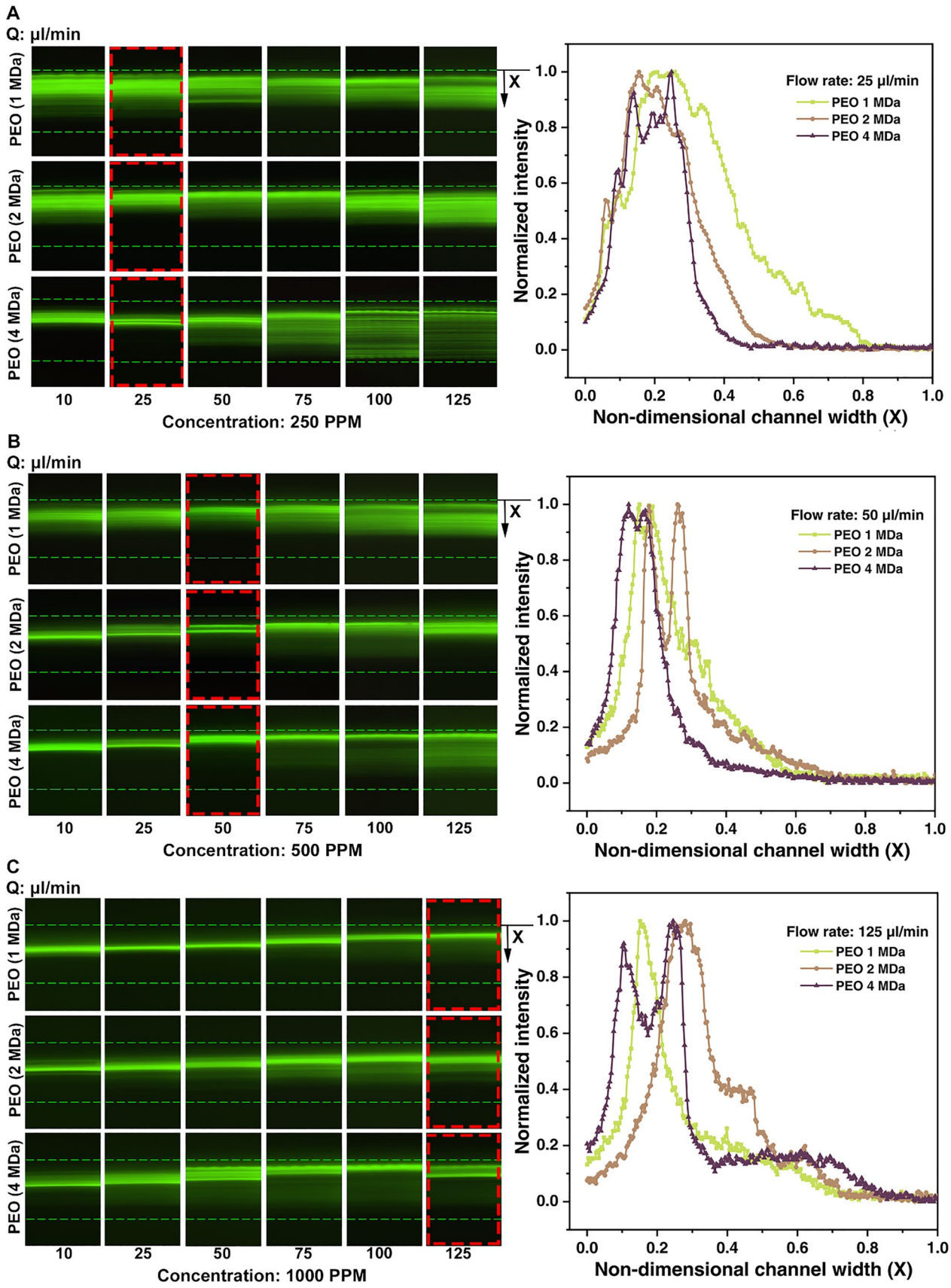
A
Q: µl/min
PEO (1 MDa)
PEO (2 MDa)
PEO (4 MDa)
10
25
50
75
100
125
Concentration: 250 PPM
X
Normalized intensity
Non-dimensional channel width (X)
Flow rate: 25 µl/min
PEO 1 MDa
PEO 2 MDa
PEO 4 MDa
B
Q: µl/min
Concentration: 500 PPM
Flow rate: 50 µl/min
C
Q: µl/min
Concentration: 1000 PPM
Flow rate: 125 µl/min

◂**Fig. 3** Focusing bands of 3 μm particles over a wide range of flow rates for PEO solutions with 1, 2, and 4 MDa molecular weights at **A** 250 ppm concentration with the normalized intensity profiles at the optimum flow rate of 25 μl/min, **B** 500 ppm concentration with the normalized intensity profiles at the optimum flow rate of 10 μl/min, and **C** 1000 ppm concentration with the normalized intensity profiles at the optimum flow rate of 125 μl/min

in the channel, which are more evident in 4 MDa solution. This issue is rooted in the fact that increasing the molecular weight intensifies the shear-thinning property and flow instabilities that cause some particles to remain dispersed, especially at high flow rates (> 100 μl/min).

4.2 Rheology effects

In clinical applications, flow rate and geometry are usually restricted to a predefined range because of the nature of the research and inherent device fabrication restrictions. Accordingly, solution rheology can be instrumental in precisely control the particle trajectory and boost the device performance. Here, the molecular weight and solution concentration are studied as the supreme rheological parameters associated with the particle migration in a non-Newtonian solution.

4.2.1 Molecular weight

To systematically evaluate the effects of molecular weight on the particle equilibrium position, focusing of 3 μm particles in 1, 2, and 4 MDa PEO solutions were tested over a wide range of flow rates. Figure 3 represents the focusing bands of the particles close to the channel outlet at 250, 500, and 1000 ppm concentrations, and the normalized intensity profiles at the optimum flow rate belonging to each concentration (25, 50, and 125 μl/min for 250, 500, and 1000 ppm, respectively). As Fig. 3A illustrates, for 250 ppm concentration, while a 1 MDa solution is unable to focus particles effectively due to the low elastic force (Wi≈3), 2 and 4 MDa solutions have tighter focusing bands at 25 μl/min. As stated in Table 1, the elastic force in 2 and 4 MDa solutions is much higher compared to the 1 MDa solution ($Wi_{2MDa}/Wi_{1MDa} \approx 5$ and $Wi_{4MDa}/Wi_{1MDa} \approx 14$ at 250 ppm concentration). Strong elasticity in 4 MDa solution results in a focusing position near the outer wall even at a low flow rate of 25 μl/min, where both Dean and inertia are negligible. With a further increase in the flow rate, the inertial force becomes more robust and pushes the particle focusing bands back towards the middle of the channel. This lateral migration is accompanied by particle dispersion for 4 MDa solution on account of the strong shear-thinning effects. The shear-thinning property modifies particle movement in two ways: increasing the inertial force due to the flow rate growth and decreasing the elastic force by reducing shear viscosity (Liu et al. 2015). It should be noted that the shear-thinning property has negligible effects when the elasticity or inertia are weak but becomes more effective as they grow (Huang and Joseph 2000). Consequently, for 4MDa solution at 75 μl/min flow rate, while Dean force and elasticity tend to focus particles near the outer wall, shear-thinning effects and inertial force precipitates particles to disperse and migrate towards the center. Figure 3A also draws a comparison between the focusing bandwidth (W_B) of the 1, 2, and 4 MDa solutions at the corresponding concentration (250 ppm) and optimum flow rate (25 μl/min). It can be deduced that, at the 250 ppm concentration, 1MDa solution is weak and tight focusing cannot be accomplished since the Wi_{1MDa}/wi_{4MDa} is almost 2.5.

4.2.2 Solution concentration

Elasticity can be controlled by adjusting either the concentration or polymer molecular weight. Since the effects of molecular weight were evaluated in the previous section "Molecular weight", this section will elaborate on the effects of concentration on the elasticity by analyzing 500 and 1000 ppm solutions. As can be seen in Fig. 3B, by increasing the concentration to 500 ppm, the particle focusing for all molecular weights and flow rates is strengthened, showing that the elastic force regulates the lateral migration of particles with greater effectiveness. However, in 1 MDa solution, a tight focusing not occurred due to the insufficient elastic force ($Wi_{avg} \approx 5$). Whereas, in 4 MDa solution, particles start to focus tightly even at a low flow rate of 10 μl/min (Wi≈10). Apparently, by increasing the flow rate, Dean drag intensifies ($De_{Q=50}/De_{Q=10} = 5$) and gently shifts the focusing band towards the outer wall in 2 and 4 MDa solutions. Focusing bands in 2 and 4 MDa solutions remain fixed till the flow rate of 50 μl/min, and start to disperse by exceeding this flow rate due to the opposing inertial and shear-thinning effects. Normalized intensity profiles along the channel width clearly express the focusing efficiency of 4 MDa solution at the flow rate of 50 μl/min. As shown in Fig. 3B, $Wi_{1MDa}/Wi_{4MDa} \approx 5$ and $Wi_{2MDa}/Wi_{4MDa} \approx 5$ are close to 2 and 1, respectively. This shows the capability of 4 MDa solution for particle sorting at very low flow rates.

Figure 3C illustrates that the particle focusing at 1000 ppm concentration is significantly improved for the 1 MDa solution, while it deteriorates the performance of 2 and 4 MDa solutions because of the strong shear-thinning effects and flow instabilities. Tight focusing in the 1 MDa solution begins at Q = 10 μl/min and continues until 125 μl/min, with shifting towards the outer wall due to the reduction in Dean drag force. Additionally, a tight focusing at this high flow rate indicates the shear-thinning effects are negligible in the 1 MDa solution. A weak focusing in 2 and 4 MDa solutions also unfolds that shear-thinning and flow instabilities

dampen the effectiveness of elastic and inertial forces. The tightest focusing bands for 2 and 4 MDa solutions in spiral channels were found at 500 ppm concentration. Although increasing the molecular weight and concentration intensifies the elasticity and shear-thinning effects, concentration has less influence on the shear-thinning property.

4.3 Extending our understanding to demonstrate position-adjustable and size-tunable particles and cells focusing

Rapid and precise manipulation of cells and particles is a demanding but indispensable task for a wide variety of applications, ranging from clinical research to biological studies. Following a systematic examination of the effects of molecular weight and concentration on the particle migration in previous sections, the optimum conditions for achieving a tight focusing band were obtained (250 ppm 1 MDa solution at flow rates of 50 and 125 µl/min, and 500 ppm 4 MDa solution at flow rates of 10 and 50 µl/min). Benefiting from the optimum conditions, we expand our knowledge by investigating the focusing position of different cells and particles of different sizes, including Saccharomyces cerevisiae (yeast) cells (~ 3 µm), red blood cells (~ 6 µm), and HeLa cells (~ 17 µm) to indicate the capability of the tuned elasto-inertial devices for cell sorting over a wide range of flow rates. Afterwards, we tried to provide a general framework for using the non-Newtonian solutions with proper concentration considering the particle and cell size. In the rectangular (200 µm × 70 µm) spiral microchannel, the cells are injected and closely focused due to the synergetic effects of elasticity, inertia, and Dean forces. Figure 4 A indicates focused cells at the channel outlet under different rheological and flow conditions. Straightforwardly, cells are well focused at low and high flow rates of 10 and 125 µl/min for 4 and 1 MDa solutions, respectively. For 1 MDa solution, cells were precisely focused at the channel outer half region at 50 µl/min flow rate and shift towards the outer wall when the flow rate is reaching 125 µl/min. Moreover, cells in 4 MDa solution focus tightly at a flow rate of 10 µl/min, showing the possibility of high-molecular-weight PEO solutions for low-velocity applications. Likewise, tight focusing close to the outer wall makes the device suitable for cell separation and purification at low flow rates. The presented microfluidic device can also focus bigger cells (> 17 µm) benefiting from the optimum flow rates and solutions rheology. Furthermore, by adjusting the channel size to the width and height of 150 × 50 µm and 90 × 30 µm, while 2 µm particles focused effectively in the middle of the channel, 1 µm particles remained slightly defocused at their optimum flow rate and solution rheology. The results clearly insist on the importance of tuning the elasticity, inertia, and Dean forces in a spiral microchannel to achieve a tight band focusing on cell/particles of different size. To conclude, PEO solutions with high molecular weight and low concentration are appropriate for those applications which require particle focusing at low flow rates; while the strong shear-thinning effects should be considered. Furthermore, low molecular weight and highly concentrated solutions are potential options for high-throughput applications.

After proceeding the cells through the device in PEO solution, we characterize the cells with flow cytometer and culture them on 12 well plate to observe cell growth. Figure 5A indicates the flow cytometry and cell viability results for different experiment group after passing through the channels in the PEO solution. Cells suspended in the 1MDa PEO solution have indistinguishable viability compared to the control group, which was cells suspended in DPBS without proceeding through the device. Changing of flow rate has a negligible impact on the viability (Fig. 5A). However, the cells suspended in 4MDa PEO solution have a dramatic decline in viability. This decline may be caused by the higher stress affecting the cells due to the higher elastic force in this solution. Figure 5B shows the area covered by reseeded cells in the 12 well plate over time. The results suggest that the proliferation rate of the cells suspended in 1MDa PEO solution is not affected. The cells are not damaged by either the shear rate or the chemical properties of Non-Newtonian solutions. Although 4MDa group has a lower cell coverage area compared to the other two groups, the slope of the cell coverage increased overtime and got close to other groups in the last day, showing a recovering growth rate after a few days. In other words, the impact on growth rate is reversible and the cells recovered within one passage. The cells were cultured up to 3 days after the experiment. The indistinguishable cell morphology in the experimental groups and the control group (Fig. 5C), showed that the cells retained their normal phenotype and metabolism.

5 Conclusion

In this study, focusing of various cells and particles through a spiral channel under different rheological conditions was explored over a wide range of flow rates to examine the fundamental of focusing behavior in a Dean-coupled elasto-inertial microchannel. Furthermore, the effects of molecular weight and solution concentration on the focusing phenomenon were investigated thoroughly. For the first time, cells/particles of different sizes (≥ 2 µm) were sharply focused at a high flow rate of 125 µl/min, confirming the suitability of Dean-coupled elasto-inertial microchannels for manipulation of particles and cells of different sizes. Results indicated that cell/particle could be strictly focused at very low (10 µl/min) and high flow rate (125 µl/min) by accurately tuning the elasticity,

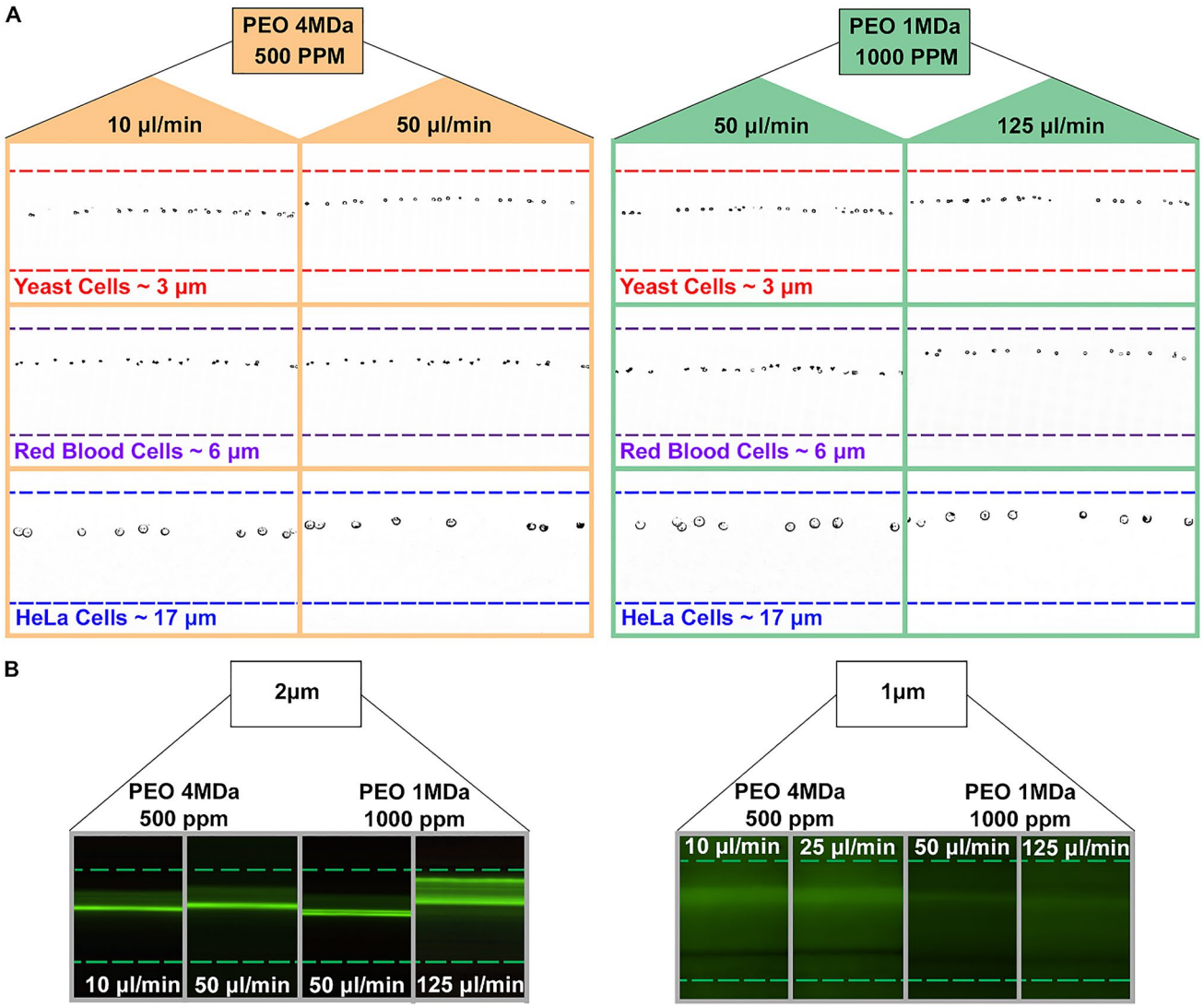

Fig. 4 **A** Tight focusing of the yeast, RBC, and Hela cells under optimum rheological and flow conditions (flow rates of 10 and 50 µl/min for the 500 ppm PEO 4MDa, and flow rates of 50 and 125 µl/min for the 1000 ppm PEO 1MDa). Cells tend to focus near the outer wall at high flow rates while shift towards the central region at low and moderate flow rates. **B** Tight focusing of the 1 and 2 µm particles under optimum rheological and flow conditions (flow rates of 10 and 50 µl/min for the 500 ppm PEO 4MDa, and flow rates of 50 and 125 µl/min for the 1000 ppm PEO 1MDa)

inertia, and Dean forces. As presented, elasticity was intensified by increasing either solution concentration or polymer molecular weight, and the shear-thinning property strengthened negatively by increasing the elasticity. Obtaining the optimum condition in which the elastic force dominates the opposing shear-thinning effects is of utmost importance. Our results revealed that the concentration of solutions has an insignificant effect on the shear-thinning property compared with the molecular weight. It can be concluded that for applications requiring particle sorting at low flow rates, PEO solutions with high molecular weight and low concentration are entirely satisfactory; yet their usage at high flow rates is hampered by strong shear-thinning effects. However, for high-throughput applications, low molecular weight and highly concentrated solutions are highly appropriate. Finally, the aim was to shed light on the fundamentals of particle migration in Dean-flow-coupled elasto-inertial devices and document the effects of solution rheology on focusing phenomena of particles.

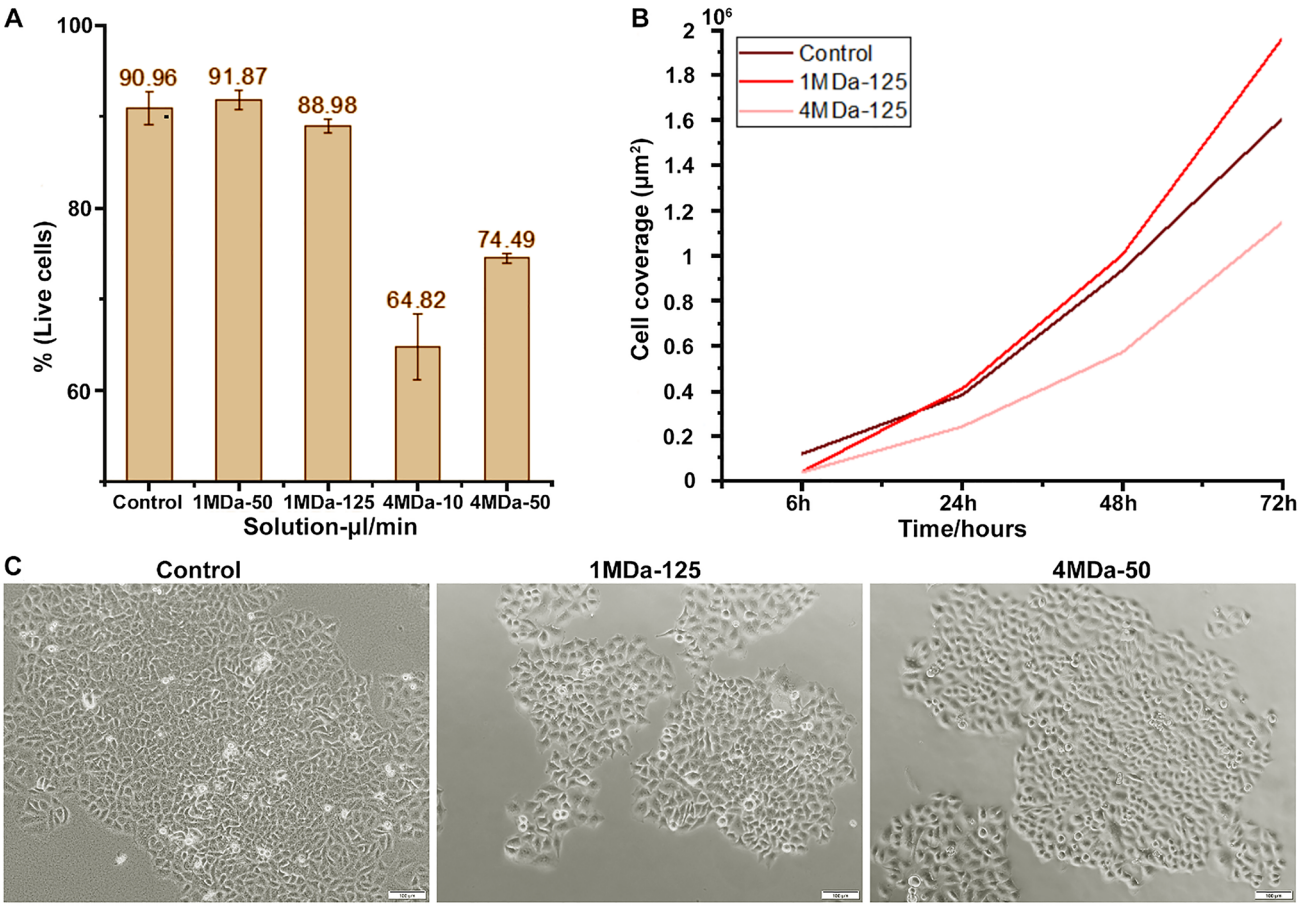

Fig. 5 **A** cell viability under optimum rheological and flow rate conditions (10 and 50 µl/min for the 500 ppm PEO 4MDa, and 50 and 125 µl/min for the 1000 ppm PEO 1MDa). **B** Growth rate of the cells for the control sample, 1MDa sample and 4MDa sample (the control sample was cultured without passing through the device, whereas 1MDa and 4MDa samples were cultured after passing at the flow rates of 50 and 125 µl/min). Three samples were counted and seeded in a 12-well plate, and the pictures of the cells were recorded every 24 h. The area covered by cells was measured by ImageJ to evaluate the growth rate of cells. **C** Cells morphology for the control sample, 1MDa sample and 4MDa sample (the control sample was cultured without passing through the device, whereas 1MDa and 4MDa samples were cultured after passing at the flow rates of 50 and 125 µl/min). The cells were cultured up to 3 days after the experiment, and the cell morphologies are depicted

Acknowledgements M.E.W. would like to acknowledge the support of the Australian Research Council through Discovery Project Grants (DP170103704 and DP180103003) and the National Health and Medical Research Council through the Career Development Fellowship (APP1143377).

References

Ahn SW, Lee SS, Lee SJ, Kim JM (2015) Microfluidic particle separator utilizing sheathless elasto-inertial focusing. Chem Eng Sci 126:237–243

Bazaz SR, Rouhi O, Raoufi MA, Ejeian F, Asadnia M, Jin D et al (2020) 3D printing of inertial microfluidic devices. Sci Rep 10(1):1–14

Bird RB, Armstrong RC, Hassager O (1987) Dynamics of polymeric liquids. Vol. 1: Fluid mechanics

Holzner G, Stavrakis S, DeMello A (2017) Elasto-inertial focusing of mammalian cells and bacteria using low molecular, low viscosity PEO solutions. Anal Chem 89(21):11653–11663

Huang P, Feng J, Hu HH, Joseph DD (1997) Direct simulation of the motion of solid particles in Couette and Poiseuille flows of viscoelastic fluids. J Fluid Mech 343:73–94

Huang P, Joseph D (2000) Effects of shear thinning on migration of neutrally buoyant particles in pressure driven flow of Newtonian and viscoelastic fluids. J Nonnewton Fluid Mech 90(2–3):159–185

Iyengar SN, Kumar T, Måertensson G, Russom A (2021) High resolution bacterial separation from blood using elasto-inertial microfluidics. Authorea Preprints

Kim MJ, Youn JR, Song YS (2018) Focusing manipulation of microalgae in a microfluidic device using self-produced macromolecules. Lab Chip 18(7):1017–1025

Kim MJ, Youn JR, Song YS (2019) Autonomous cell sorting using self-secreted macromolecules. Microfluid Nanofluid 23(10):115

Kumar T, Ramachandraiah H, Iyengar SN, Banerjee I, Mårtensson G, Russom A (2021) High throughput viscoelastic particle focusing and separation in spiral microchannels. Sci Rep 11(1):1–13

Lee DJ, Brenner H, Youn JR, Song YS (2013) Multiplex particle focusing via hydrodynamic force in viscoelastic fluids. Sci Rep 3:3258

Leshansky AM, Bransky A, Korin N, Dinnar UJ (2007) Tunable nonlinear viscoelastic "focusing" in a microfluidic device. Phys Rev Lett 98(23):234501

Liu C, Ding B, Xue C, Tian Y, Hu G, Sun J (2016) Sheathless focusing and separation of diverse nanoparticles in viscoelastic solutions with minimized shear thinning. Anal Chem 88(24):12547–12553. https://doi.org/10.1021/acs.analchem.6b04564

Liu C, Guo J, Tian F, Yang N, Yan F, Ding Y et al (2017) Field-free isolation of exosomes from extracellular vesicles by microfluidic viscoelastic flows. ACS Nano 11(7):6968–6976. https://doi.org/10.1021/acsnano.7b02277

Liu K, Yang Q, Chen F, Zhao Y, Meng X, Shan C et al (2015) Design and analysis of the cross-linked dual helical micromixer for rapid mixing at low Reynolds numbers. Microfluid Nanofluid 19(1):169–180

Lu X, Chow JJM, Koo SH, Jiang B, Tan TY, Yang D et al (2021) Sheathless and high-throughput elasto-inertial bacterial sorting for enhancing molecular diagnosis of bloodstream infection. Lab Chip 21(11):2136–2177

Mihandoust A, Razavi Bazaz S, Maleki-Jirsaraei N, Alizadeh M, Taylor RA, Ebrahimi Warkiani M (2020) High-throughput particle concentration using complex cross-section microchannels. Micromachines. https://doi.org/10.3390/mi11040440

Moloudi R, Oh S, Yang C, Warkiani ME, Naing MW (2018) Inertial particle focusing dynamics in a trapezoidal straight microchannel: application to particle filtration. Microfluid Nanofluid 22(3):33

Nikdoost A, Rezai P (2020) Dean flow velocity of viscoelastic fluids in curved microchannels. AIP Adv 10(8):085015

Raoufi MA, Mashhadian A, Niazmand H, Asadnia M, Razmjou A, Warkiani ME (2019) Experimental and numerical study of elasto-inertial focusing in straight channels. Biomicrofluidics 13(3):034103

Raoufi MA, Razavi Bazaz S, Niazmand H, Rouhi O, Asadnia M, Razmjou A et al (2020) Fabrication of unconventional inertial microfluidic channels using wax 3D printing. Soft Matter 16(10):2448–2459. https://doi.org/10.1039/C9SM02067E

Razavi Bazaz S, Amiri HA, Vasilescu S, Abouei Mehrizi A, Jin D, Miansari M et al (2020a) Obstacle-free planar hybrid micromixer with low pressure drop. Microfluid Nanofluid 24(8):61. https://doi.org/10.1007/s10404-020-02367-x

Razavi Bazaz S, Mashhadian A, Ehsani A, Saha SC, Krüger T, Ebrahimi Warkiani M (2020b) Computational inertial microfluidics: a review. Lab Chip 20(6):1023–1048. https://doi.org/10.1039/C9LC01022J

Razavi Bazaz S, Kashaninejad N, Azadi S, Patel K, Asadnia M, Jin D et al (2019) Rapid softlithography using 3D-printed molds. Adv Mater Technol 4(10):1900425

Rodd LE, Scott TP, Boger DV, Cooper-White JJ, McKinley GH (2005) The inertio-elastic planar entry flow of low-viscosity elastic fluids in micro-fabricated geometries. J Nonnewton Fluid Mech 129(1):1–22

Rodd L, Cooper-White J, Boger D, McKinley G (2007) Role of the elasticity number in the entry flow of dilute polymer solutions in micro-fabricated contraction geometries. J Nonnewton Fluid Mech 143(2–3):170–191

Rzhevskiy SA, Razavi Bazaz S, Ding L, Kapitannikova A, Sayyadi N, Campbell D et al (2020) Rapid and label-free isolation of tumour cells from the urine of patients with localised prostate cancer using inertial microfluidics. Cancers. https://doi.org/10.3390/cancers12010081

Seo KW, Byeon HJ, Huh HK, Lee SJ (2014a) Particle migration and single-line particle focusing in microscale pipe flow of viscoelastic fluids. RSC Adv 4(7):3512–3520. https://doi.org/10.1039/C3RA43522A

Seo KW, Kang YJ, Lee SJ (2014b) Lateral migration and focusing of microspheres in a microchannel flow of viscoelastic fluids. Physics Fluids 26(6):063301

Shrestha J, Ghadiri M, Shanmugavel M, Razavi Bazaz S, Vasilescu S, Ding L et al (2019) A rapidly prototyped lung-on-a-chip model using 3D-printed molds. Organs-on-a-Chip 1:100001. https://doi.org/10.1016/j.ooc.2020.100001

Song HY, Lee SH, Salehiyan R, Hyun K (2016) Relationship between particle focusing and dimensionless numbers in elasto-inertial focusing. Rheolgica Acta 55(11):889–900. https://doi.org/10.1007/s00397-016-0962-3

Tang W, Fan N, Yang J, Li Z, Zhu L, Jiang D et al (2019) Elasto-inertial particle focusing in 3D-printed microchannels with unconventional cross sections. Microfluid Nanofluid 23(3):1–10

Tang D, Chen M, Han Y, Xiang N, Ni Z (2021) Asymmetric serpentine microchannel based impedance cytometer enabling consistent transit and accurate characterization of tumor cells and blood cells. Sensors Actuators b: Chemical 336:129719

Tirtaatmadja V, McKinley GH, Cooper-White JJ (2006) Drop formation and breakup of low viscosity elastic fluids: effects of molecular weight and concentration. Physics Fluids 18(4):043101

Villone M, Davino G, Hulsen M, Greco F, Maffettone P (2013) Particle motion in square channel flow of a viscoelastic liquid: migration vs. secondary flows. J Non-Newtonian Fluid Mech 195:1–8

Warkiani ME, Tay AKP, Guan G, Han J (2015a) Membrane-less microfiltration using inertial microfluidics. Sci Rep 5:11018

Warkiani ME, Wu L, Tay AKP, Han J (2015b) Large-volume microfluidic cell sorting for biomedical applications. Ann Rev Biomed Eng 17(1):34

Xiang N, Ni Z, Yi H (2018) Concentration-controlled particle focusing in spiral elasto-inertial microfluidic devices. Electrophoresis 39(2):417–424

Xiang N, Dai Q, Ni Z (2016a) Multi-train elasto-inertial particle focusing in straight microfluidic channels. Phys Lett 109(13):134101

Xiang N, Zhang X, Dai Q, Cheng J, Chen K, Ni Z (2016b) Fundamentals of elasto-inertial particle focusing in curved microfluidic channels. Lab Chip 16(14):2626–2635

Yang S, Kim JY, Lee SJ, Lee SS, Kim JM (2011) Sheathless elasto-inertial particle focusing and continuous separation in a straight rectangular microchannel. Lab Chip 11(2):266–273

Yuan D, Sluyter R, Zhao Q, Tang S, Yan S, Yun G et al (2019) Dean-flow-coupled elasto-inertial particle and cell focusing in symmetric serpentine microchannels. Microfluid Nanofluid 23(3):41

Zhou Y, Ma Z, Ai Y (2020) Dynamically tunable elasto-inertial particle focusing and sorting in microfluidics. Lab Chip 20(3):568–581